Nonlinearity **13** (2000) 1411–1423. Printed in the UK PII: S0951-7715(00)10432-3

Dispersion and collapse of wave maps

Piotr Bizoń†, Tadeusz Chmaj‡ and Zbisław Tabor†

† Institute of Physics, Jagellonian University, Kraków, Poland
‡ Institute of Nuclear Physics, Kraków, Poland

Received 16 December 1999, in final form 22 May 2000
Recommended by N Manton

Abstract. We study numerically the Cauchy problem for equivariant wave maps from 3 + 1 Minkowski spacetime into the 3-sphere. On the basis of numerical evidence combined with stability analysis of self-similar solutions we formulate two conjectures. The first conjecture states that singularities which are produced in the evolution of sufficiently large initial data are approached in a universal manner given by the profile of a stable self-similar solution. The second conjecture states that the codimension-one stable manifold of a self-similar solution with exactly one instability determines the threshold of singularity formation for a large class of initial data. Our results can be considered as a toy-model for some aspects of the critical behaviour in the formation of black holes.

AMS classification scheme numbers: 35L67, 35L70, 35Q75

1. Introduction

Let M be a spacetime with metric η and N be a complete Riemannian manifold with metric g. The wave map $U : M \to N$ is defined as a critical point of the action

$$S(U) = \int_M g_{AB}\, \partial_a U^A \partial_b U^B \eta^{ab}\, \mathrm{d}V_M\,. \tag{1}$$

The associated Euler–Lagrange equations constitute the system of semilinear wave equations

$$\Box_\eta U^A + \Gamma^A_{BC}(U)\partial_a U^B \partial^a U^C = 0, \tag{2}$$

where the Γs are the Christoffel symbols of the target metric g.

The recent surge of interest in wave maps (known in the physics literature as σ-models) stems from the fact that they provide an attractive toy-model for more complicated relativistic field equations. In particular they share some features with the Einstein equations so understanding the problems of global existence and formation of singularities for wave maps may shed some light on the analogous, but much more difficult, problems in general relativity. Having this analogy in mind we have studied the Cauchy problem for equation (2) in the case where the domain manifold is $3+1$ Minkowski spacetime, $M = \mathbb{R}^{3+1}$, and the target manifold is the 3-sphere, $N = S^3$. Although our primary motivation was an attempt to get insight into some aspects of critical behaviour in gravitational collapse, we think that our results are interesting in their own right. In this paper we restrict attention to equivariant maps. In polar coordinates on $\mathbb{R}^{3+1}$ and S^3 the respective metrics are

$$\eta = -\mathrm{d}t^2 + \mathrm{d}r^2 + r^2\mathrm{d}\omega^2, \quad g = \mathrm{d}u^2 + \sin^2(u)\mathrm{d}\Omega^2, \tag{3}$$

0951-7715/00/041411+13$30.00

where $d\omega^2$ and $d\Omega^2$ are the standard metrics on S^2. Equivariant maps have the form

$$U(t, r, \omega) = (u(t, r), \Omega(\omega)), \tag{4}$$

where Ω is a homogeneous harmonic polynomial of degree $l > 0$. In what follows we consider the case $l = 1$, where $\Omega = \omega$ (such maps are called corotational). For a corotational map the Cauchy problem for equation (2) reduces to the semilinear wave equation

$$u_{tt} = u_{rr} + \frac{2}{r}u_r - \frac{\sin(2u)}{r^2} \tag{5}$$

with smooth initial data

$$u(0, r) = \phi(r), \quad u_t(0, r) = \psi(r). \tag{6}$$

Regularity at the origin requires that the initial data vanish at $r = 0$ which implies the boundary condition $u(t, 0) = 0$ for all $t < T$, where T is a time when the first singularity (if there is any) develops at $r = 0$. The requirement that the conserved energy associated with solutions of (5)

$$E[u] = \frac{1}{2}\int_0^\infty (r^2u_t^2 + r^2u_r^2 + 2\sin^2 u)\mathrm{d}r \tag{7}$$

is finite imposes a boundary condition at spatial infinity $u(t, \infty) = k\pi$ $(k = 0, 1, \ldots)$, where an integer k is the topological degree of the map. Since the time evolution is continuous (at least for $t < T$), this condition breaks the Cauchy problem into infinitely many disconnected sectors labelled by the degree k.

Note that the energy scales as $E[u(x/\lambda)] = \lambda E[u(x)]$ which means that equation (5) is supercritical (like Einstein's equations). It is widely believed that for supercritical equations the solutions with sufficiently small initial data exist for all times while large data solutions develop singularities in finite time [7]. In the case of (5) the global existence for small (in the Sobolev space H^k with sufficiently large k) data was proved by Kovalyov [8] and Sideris [11]. For large data there are no rigorous results, however it is known that there exist smooth data which lead to blowup in finite time. An example of such data is due to Shatah who showed that (5) admits a self-similar solution $u(t, r) = f_0(\frac{r}{T-t})$ which is perfectly smooth for $t < T$ but breaks down at $t = T$. Turok and Spergel [13] found this solution in closed form $f_0 = 2\arctan(\frac{r}{T-t})$ so in the following we will refer to f_0 as the TS solution. Note that for $t < T$, the TS solution has degree $k = 1$.

On the basis of our numerical simulations we conjecture that the example of blowup given by Shatah is generic. By this we mean that there is a large open set of initial data which blow up in a finite time T and the asymptotic shape of solutions near the blowup point $(r = 0)$ approaches $f_0(\frac{r}{T-t})$ as $t \to T^-$. In this sense the blowup can be considered as local convergence to the TS solution f_0. Actually, our failed efforts to produce a non-self-similar singularity lead us to suspect that the blowup is universally self-similar. Note that the self-similarity of blowup excludes a concentration of energy at the singularity and suggests that the solutions can be continued beyond the blowup time in an almost continuous fashion. We must admit that this aspect of singularity formation for wave maps is somewhat disappointing from the standpoint of modelling the formation of energy trapping singularities (like black holes).

Whenever the singularities develop from some but not all data, there arises a natural question of determining the threshold of singularity formation. We investigated this issue using a basic technique of evolving various one-parameter families of initial data which interpolate between global existence (dispersion) and blowup. Along each such family there exists a point (critical initial data) which separates the two regimes. We show that the critical initial data blow up in a finite time T and the asymptotic shape of solutions near the blowup point $(r = 0)$

approaches $f_1(\frac{r}{T-t})$, a self-similar solution with one unstable mode. The marginally critical data approach f_1 for intermediate times but eventually the unstable mode becomes dominant and ejects the solutions towards dispersion or stable blowup (that is, f_0). Thus, we conjecture that the codimension-one stable manifold of the solution f_1 plays the role of the threshold of singularity formation for a large set of initial data.

The threshold behaviour in our model is similar to the type II critical behaviour in gravitational collapse (see [5] for a recent review) where self-similar solutions of Einstein's equations (continuous or discrete, depending on a model) sit at the threshold of formation of a black hole. There are also many parallels between our results and the work of Brenner et al [4] on the chemotaxis equation. All that suggests that self-similar behaviour at the threshold of singularity formation is a common feature for evolutionary partial differential equations†.

The rest of the paper is organized as follows. In the next two sections we discuss some special solutions of (5) which are potential candidates for attractors. In section 2 we analyse self-similar solutions and their linear stability. Section 3 is devoted to static solutions. In section 4 we describe the results of numerical simulations and document the numerical evidence behind the two conjectures formulated above.

2. Self-similar solutions

Note that equation (5) is invariant under dilations: if $u(t, r)$ is a solution, so is $u_a(t, r) = u(at, ar)$. It is thus natural to look for self-similar solutions of the form

$$u(t, r) = f\left(\frac{r}{T-t}\right), \tag{8}$$

where T is a positive constant. Substituting the ansatz (8) into (5) we obtain the ordinary differential equation

$$f'' + \frac{2}{\rho} f' - \frac{\sin(2f)}{\rho^2(1-\rho^2)} = 0, \tag{9}$$

where $\rho = r/(T-t)$ and $' = \mathrm{d}/\mathrm{d}\rho$. For $t < T$ we have $0 \leqslant \rho < \infty$.

It is sufficient to consider equation (9) only inside the past light cone of the point $(T, 0)$, that is for $\rho \in [0, 1]$. The regularity of solutions at the endpoints of this interval enforces the following behaviour

$$f(\rho) \sim a\rho \quad \text{as} \quad \rho \to 0, \tag{10}$$

and

$$f(\rho) \sim \frac{\pi}{2} + b(1-\rho) \quad \text{as} \quad \rho \to 1, \tag{11}$$

where a and b are arbitrary constants. At each endpoint the parameters a and b determine unique local solutions. One can show that there is a countable sequence of pairs (a_n, b_n) for which the corresponding solutions, denoted by $f_n(\rho)$, are globally regular in the sense that they satisfy both boundary conditions (10) and (11) and are smooth for $\rho \in (0, 1)$.

These solutions can be smoothly extended for $\rho > 1$ by solving (9) with the initial condition (11). One can show that the asymptotic behaviour for $\rho \to \infty$ is

$$f_n(\rho) \sim c_n + \frac{d_n}{\rho} + O\left(\frac{1}{\rho^2}\right), \tag{12}$$

† There is a vast literature on a related problem for the nonlinear Schrödinger equation. See [12] for a recent review and bibliography of this subject.

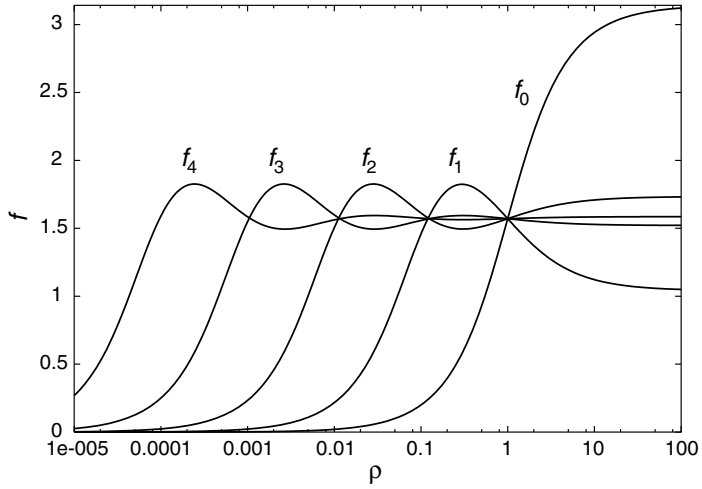

Figure 1. The first five self-similar solutions.

Table 1. The parameters of solutions shown in figure 1.

n	0	1	2	3	4
a_n	2	21.757 413	234.501 47	2522.0683	27 113.388
b_n	1	−0.305 664	0.093 2163	−0.028 4312	0.008 6717

where $c_n \to \pi/2$ as $n \to \infty$. The countable family f_n was discovered numerically by Äminneborg and Bergström [1]; recently its existence was proven rigorously via a shooting argument [3]. The integer index $n = 0, 1, \ldots$ denotes the number of intersections of $f_n(\rho)$ with the line $f = \pi/2$ on the interval $\rho \in [0, 1)$. The 'ground state' solution of this family is the TS solution $f_0 = 2\arctan(\rho)$. The solutions f_n with $n > 0$ can be obtained numerically by a standard shooting-to-a-fitting-point technique, that is by integrating equation (9) away from the singular points $\rho = 0$ and $\rho = 1$ in the opposite directions with some trial parameters a and b and then adjusting these parameters so that the solution joins smoothly at the fitting point. The profiles of solutions generated in this way (for $n \leqslant 4$) are shown in figure 1; the corresponding parameters (a_n, b_n) are given in table 1.

The role of self-similar solutions f_n in the evolution depends crucially on their stability with respect to small perturbations. In order to analyse the linear stability of the self-similar solutions it is convenient to define the new time coordinate $\tau = -\ln(T - t)$ and rewrite equation (5) in terms of τ and ρ

$$u_{\tau\tau} + u_\tau + 2\rho\, u_{\rho\tau} - (1-\rho^2)\left(u_{\rho\rho} + \frac{2}{\rho}u_\rho\right) + \frac{\sin(2u)}{\rho^2} = 0. \tag{13}$$

The standard procedure is to seek solutions of (13) in the form $u(\tau, \rho) = f_n(\rho) + w(\tau, \rho)$. Neglecting the $O(w^2)$ terms we obtain a linear evolution equation for the perturbation $w(\tau, \rho)$

$$w_{\tau\tau} + w_\tau + 2\rho\, w_{\rho\tau} - (1-\rho^2)\left(w_{\rho\rho} + \frac{2}{\rho}w_\rho\right) + \frac{2\cos(2f_n)}{\rho^2}w = 0. \tag{14}$$

Substituting $w(\tau, \rho) = \mathrm{e}^{\lambda\tau} v_\lambda(\rho)/\rho$ into (14) we get an eigenvalue problem

$$-(1-\rho^2)v_\lambda'' + 2\lambda\rho v_\lambda' + \lambda(\lambda-1)v_\lambda + \frac{2\cos(2f_n)}{\rho^2}v_\lambda = 0. \tag{15}$$

Near $\rho = 0$ the leading behaviour of solutions of (15) is $v_\lambda(\rho) \sim \rho^\alpha$ where $\alpha(\alpha - 1) = 2$, so to ensure regularity we require

$$v_\lambda(\rho) \sim \rho^2 \quad \text{as} \quad \rho \to 0. \tag{16}$$

Near $\rho = 1$ the leading behaviour is $v_\lambda(\rho) \sim (1-\rho)^\beta$ where $\beta(\beta - 1 + \lambda) = 0$. The behaviour corresponding to $\beta = 1 - \lambda$ is not admissible (unless $\lambda = 1$), so regular solutions must have $\beta = 0$. Then we have (up to a normalization constant)

$$v_\lambda(\rho) \sim 1 + \frac{2 + \lambda(1-\lambda)}{2\lambda}(1-\rho) + O((1-\rho)^2) \qquad \text{as} \quad \rho \to 1. \tag{17}$$

To find the eigenvalues we need to solve equation (15) on the interval $\rho \in [0, 1]$ with the boundary conditions (16) and (17). We did this numerically (for $n \leqslant 4$) by shooting the solutions from both ends and matching the logarithmic derivative at a midpoint. Given an eigenvalue λ, the eigenfunction $v_\lambda(\rho)$ can be extended for $\rho > 1$ by solving (15) with the initial condition (17). Our numerical results strongly suggest that the solution f_n has exactly $n+1$ positive eigenvalues (unstable modes). We denote them by $\lambda_k^{(n)}$ $(k = 1, \ldots, n+1)$ where $\lambda_1^{(n)} > \lambda_2^{(n)} > \ldots > \lambda_{n+1}^{(n)} = 1$. For example, for $n = 1$ we have $\lambda_1^{(1)} \approx 6.333\,625$, $\lambda_2^{(1)} = 1$; for $n = 2$ we have $\lambda_1^{(2)} \approx 59.07$, $\lambda_2^{(2)} \approx 6.304$, $\lambda_3^{(2)} = 1$.

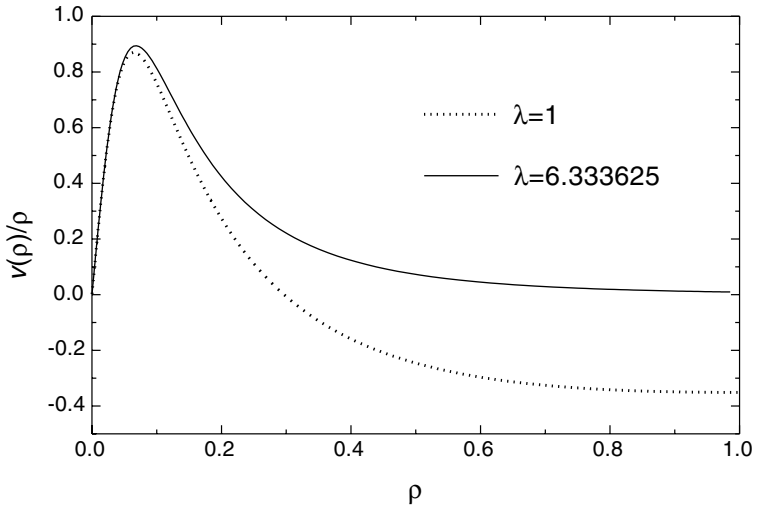

Figure 2. The profiles of unstable modes around the solution $f_1(\rho)$. The 'real' unstable mode (solid line) corresponds to the eigenvalue $\lambda_1^{(1)} \approx 6.333\,625$. The gauge mode (dotted line) has $\lambda_2^{(1)} = 1$. For better visualization both plots are normalized to the same slope at the origin.

For every n the lowest positive eigenvalue $\lambda = 1$ corresponds to the gauge mode which is due to the freedom of choosing the blowup time T. To see this, consider a solution $f_n(r/(T' - t))$. In terms of the similarity variables $\tau = -\ln(T - t)$ and $\rho = r/(T - t)$, we have

$$f_n\left(\frac{r}{T' - t}\right) = f_n\left(\frac{\rho}{1 + \epsilon \mathrm{e}^\tau}\right) \quad \text{where} \quad \epsilon = T' - T. \tag{18}$$

In other words, each self-similar solution $f_n(\rho)$ generates the orbit of solutions of (13) $f_n(\frac{\rho}{1+\epsilon \mathrm{e}^\tau})$. It is easy to verify that the generator of this orbit

$$w(\tau, \rho) = -\frac{\mathrm{d}}{\mathrm{d}\epsilon}\, f_n\left(\frac{\rho}{1 + \epsilon \mathrm{e}^\tau}\right)\bigg|_{\epsilon=0} = \mathrm{e}^\tau \rho f_n'(\rho) \tag{19}$$

satisfies (14), thus $v_n = f_n'(\rho)$ satisfies (15) with $\lambda = 1$. Note that this eigenfunction has exactly n zeros on $\rho \in (0, 1)$ (since f_n has n extrema). For a standard Sturm–Liouville problem this would imply the existence of n eigenvalues above $\lambda = 1$. It was shown in [3] that a similar result holds in the case of (15), in agreement with our numerical findings.

3. Static solutions

Static solutions of equation (5) can be interpreted as spherically symmetric harmonic maps from the Euclidean space $\mathbb{R}^3$ into S^3. They satisfy the ordinary differential equation

$$u'' + \frac{2}{r}u' - \frac{\sin(2u)}{r^2} = 0, \tag{20}$$

where now $' = \mathrm{d}/\mathrm{d}r$. The obvious constant solutions of (20) are $u = 0$ and $u = \pi$; geometrically these are maps into the north and the south pole of S^3, respectively. The energy of these maps attains a global minimum $E = 0$. Another constant solution is the equator map $u = \pi/2$, but this solution is singular and has infinite energy. The scale invariance of (20) excludes existence of nontrivial regular solutions with finite energy. However, there exists a regular solution with infinite energy, denoted here by $u_S(r)$, which behaves as

$$u_S(r) \sim \begin{cases} r & \text{for } r \to 0, \\ \frac{\pi}{2} + \frac{C}{\sqrt{r}} \sin(\frac{\sqrt{7}}{2} \ln r + \delta) & \text{for } r \to \infty. \end{cases} \tag{21}$$

The existence of this solution, shown in figure 3, can be easily proven using $x = \ln(r)$ which transforms (20) into a damped pendulum equation [6].

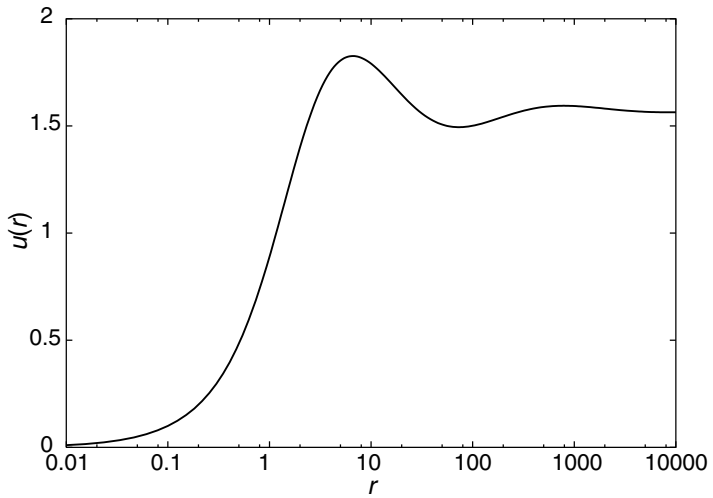

Figure 3. The static solution $u_S(r)$.

Note that by dilation symmetry, the solution $u_S(r)$ generates the orbit of static solutions $u_S^a(r) = u_S(ar)$.

We consider now the linear stability of the static solution u_S. Inserting $u(t, r) = u_S(r) + \mathrm{e}^{\mathrm{i}kt} v(r)$ into (5) and linearizing, we get the eigenvalue problem

$$-v'' - \frac{2}{r}v' + V(r)v = k^2 v, \quad V(r) = \frac{2\cos(2u_S)}{r^2}. \tag{22}$$

If the singular $1/r^2$ part is subtracted from V, then (22) becomes the p-wave radial Schrödinger equation in the regular potential $V_{reg} = V(r) - 2/r^2$. This potential has infinitely many bound states as can be shown by the following standard argument. Consider the perturbation induced by the scaling transformation

$$v(r) = \frac{\mathrm{d}}{\mathrm{d}a} u_S^a(r)\bigg|_{a=1} = r u_S'(r). \tag{23}$$

This is an eigenfunction to zero eigenvalue (so-called zero mode). Since $u_S(r)$ has infinitely many extrema, the zero mode has infinitely many nodes which implies by the standard result from Sturm–Liouville theory that there are infinitely many negative eigenvalues, and *eo ipso* infinitely many unstable modes around $u_S(r)$. We found numerically that the 'most unstable' mode has the eigenvalue $k^2 = -0.061\,306$. The spectrum of perturbations around the rescaled solutions $u_S^a(r)$ is obtained by scaling $v(r) \to v(kr)$, $k^2 \to a^2 k^2$.

To summarize, there exists the static solution $u_S(r)$ (and the continuous family of its rescalings $u_S^a(r)$) which has infinite energy and infinitely many unstable modes. Can such a beast play any role in dynamical evolution? The answer is not clear to us. The point is that both the infinite energy and infinite instability of $u_S(r)$ have an origin in the far-field behaviour so it does not seem impossible that solutions $u_S^a(r)$ truncated at some radius appear as local attractors†.

An alternative way of looking at this issue is to consider solutions of (20) in a finite region $r \leqslant R$, that is harmonic maps from a ball $B^3(R)$ into S^3. In the Dirichlet case, $u(R) = c$, the number of such solutions depends on the value of a constant c — this was discussed in detail by Jäger and Kaul [6]. In the Neumann case, $u'(R) = 0$, which might be more relevant in dynamics, there exists a countable family of finite energy regular solutions $u_k(r)$. They are given by

$$u_k(r) = u_S^{a_k}(r) \quad \text{with} \quad a_k = \frac{r_k}{R}, \tag{24}$$

where r_k is the kth Neumann point of $u_S(r)$, that is a point where $u_S'(r_k) = 0$ ($k = 1, 2, \ldots$). By construction the solution $u_k(r)$ has $k-1$ extrema on $r \in (0, R)$. By the same Sturm–Liouville theory argument as above, one can show that a truncated solution u_k has exactly $k-1$ instabilities so *a priori* it might appear as a codimension $(k-1)$ local attractor in the dynamical evolution.

In passing we remark that a similar structure of static solutions arising in the chemotaxis problem was discussed by Brenner *et al* [4].

4. Numerical results

In this section we describe the results of our numerical simulations of the Cauchy problem (5), (6). The main goal of these simulations was to identify the generic final states of evolution (stable attractors) and determine the boundaries between their basins of attraction. We emphasize that the convergence to attractors (which is due to radiation of energy to infinity) is always meant in a local sense. Before going into details, we would like to say a few words about the numerical techniques we employed. The simulations were performed by two different finite difference methods. The first method was based on an adaptive mesh refinement

† In a recent paper [9] Liebling, Hirschmann and Isenberg claim to have seen the solutions $u_S^a(r)$ at the threshold for singularity formation in the evolution of very special initial data of noncompact support. We have serious misgivings about this result, in particular we do not understand the discussion of 'critical' solutions which are not intermediate attractors.

algorithm. This code allowed us to probe the structure of solutions near the singularity with good resolution. The second method, designed especially to study the convergence to self-similar solutions, solved the Cauchy problem for equation (13) on a fixed grid. In this case there was no need of mesh refinement because the convergence to self-similar profiles is a smooth process in similarity variables. The main difficulty of using similarity variables is that we do not know the blowup time T in advance, which means that we have to deal with the gauge mode instability. To suppress this instability (that is, to guess a blowup time T) we fine-tuned an extra parameter in the initial data. The fact that the two independent numerical techniques generated basically the same outputs makes us feel confident about our results.

We recall that initial data of finite energy can be classified according to the topological degree of the wave map at a fixed time (which is a map from topological S^3 into S^3). Since the degree is preserved by evolution, the Cauchy problem breaks into infinitely many topological sectors. The nonzero degree data are not small by definition, and we conjecture that they always develop singularities. Thus, from the point of view of studying the threshold for singularity formation, only degree zero data are interesting so most of our discussion is focused to such data. A typical example is an ingoing 'Gaussian'

$$u(0,r) = \phi(r) = A\, r^3 \exp\left[-\left(\frac{r-r_0}{s}\right)^4\right], \qquad u_t(0,r) = \psi(r) = \phi'(r). \tag{25}$$

In agreement with the rigorous results of [8, 11] we found that if the initial data are sufficiently small then the solution disperses, that is it converges uniformly on any compact interval to the 'vacuum' solution $u = 0$. In contrast, large initial data develop singularities in finite time—this manifests itself in an unbounded growth of the gradient of solution at $r = 0$. The precise character of blowup will be described below.

Threshold behaviour

In order to determine the boundary between two generic asymptotic states of evolution, dispersion and collapse, we considered the evolution of various interpolating one-parameter families of initial data $(\phi(r, p), \psi(r, p))$, that is such families where the corresponding solutions exist globally if the parameter p is small and blow up if the parameter p is large. Along each interpolating family there must exist a critical parameter value p^* which separates these two regimes. Given two values p_{small} and p_{large}, it is straightforward (in principle) to find p^* by bisection. Repeating this for many different interpolating families of initial data one obtains a set of critical data which by construction belongs to the threshold. In order to figure out the structure of the threshold one needs to determine the flow of critical data. The precisely critical data cannot be prepared numerically but in practice it is sufficient to follow the evolution of marginally critical data. We found that the flow of such data has a transient phase when it seems to approach the self-similar solution $f_1(r/(T-t))$ for some T (see figure 4). This behaviour is universal in the sense that it is independent of the family of initial data; only the parameter T depends on the data.

This kind of behaviour can be naturally explained as follows. As we showed above, the self-similar solution f_1 has exactly one unstable mode (apart from the gauge mode)—in other words the stable manifold of this solution, $W_S(f_1)$, has codimension one and therefore generic one-parameter families of initial data do intersect it. The points of intersection correspond to critical initial data that converge asymptotically to f_1. The marginally critical data, by continuity, initially remain close to $W_S(f_1)$ and approach f_1 for intermediate times but eventually are repelled from its vicinity along the one-dimensional unstable manifold (see figure 5). Within this picture the universality of marginally critical dynamics in the intermediate

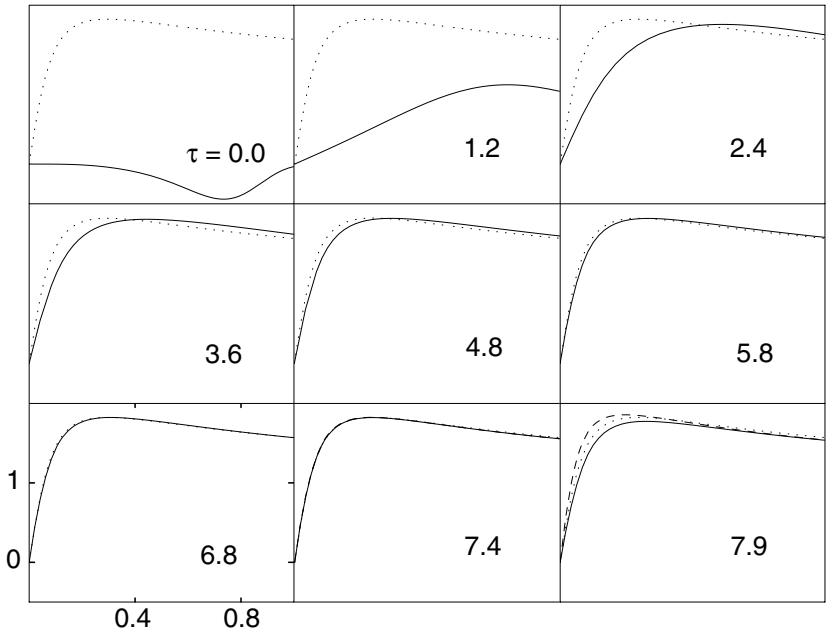

Figure 4. The plot of $u(\tau, \rho)$ against ρ from the evolution (in similarity variables) of two marginally critical Gaussian-type initial data of the form (25), one subcritical (solid line) and one supercitical (dashed line). These data are identical, except for the amplitudes which differ by 10^{-17}, so the solutions practically coincide until the last frame. The influence of the gauge mode instability is minimized by fine-tuning the width of the Gaussian. The convergence to the self-similar profile $f_1(\rho)$ (dotted line) is clearly seen. In the last frame the two solutions depart from the intermediate attractor in the opposite directions.

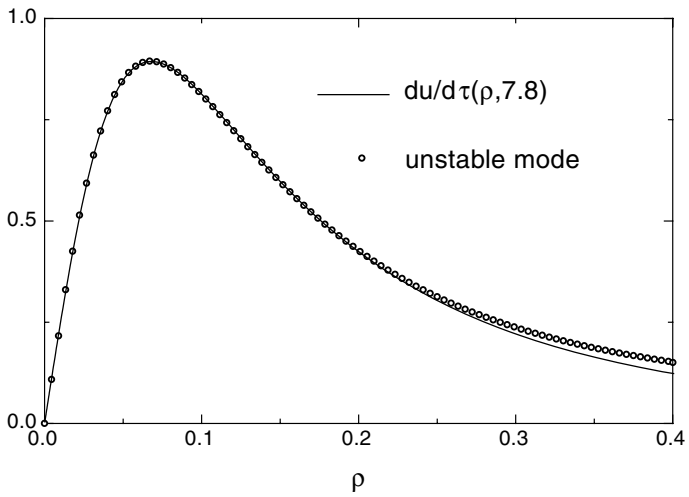

Figure 5. Departure of the supercritical solution shown in figure 4 from the intermediate attractor. The τ-derivative of the solution is shown to coincide (for small ρ) with the suitably normalized unstable mode around f_1.

asymptotics follows immediately from the fact that the same unstable mode dominates the evolution of all solutions. More precisely, the evolution of marginally critical solutions in the intermediate asymptotics can be approximated as

$$u(t,r) = f_1(\rho) + c(p)\mathrm{e}^{\lambda\tau} v(\rho)/\rho + \text{decaying modes}, \tag{26}$$

where $\rho = r/(T-t)$, $\tau = -\ln(T-t)$, and $\lambda = \lambda_1^{(1)} \approx 6.3336$. The small constant $c(p)$, which is the only vestige of the initial data, quantifies an admixture of the unstable mode—for precisely critical data $c(p^*) = 0$. The 'lifetime' τ^* of the transient phase during which the linear approximation (26) is valid is determined by the time in which the unstable mode grows to a finite size, that is $c(p)\mathrm{e}^{\lambda\tau^*} \sim O(1)$. Using $c(p) \approx c'(p^*)(p-p^*)$, this gives $\tau^* \sim -\frac{1}{\lambda}\ln|p-p^*|$.

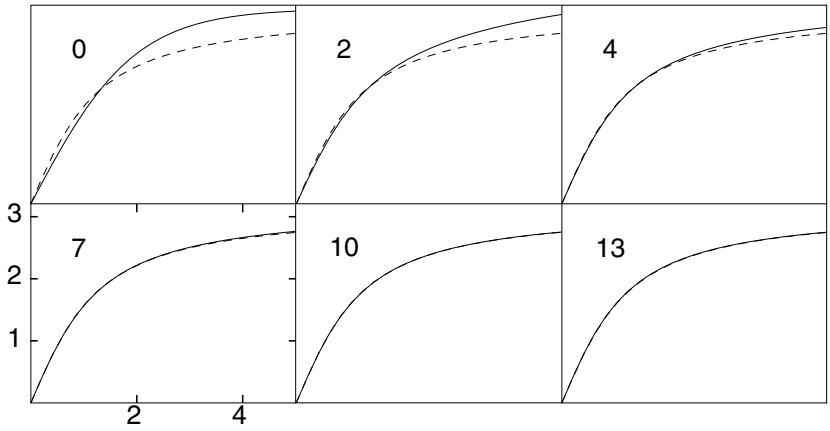

Figure 6. The evolution of kink-type initial data $u(0,\rho) = \pi\tanh(\rho/s)$ in similarity variables. The solution (solid line) converges to the Turok–Spergel solution $f_0(\frac{\rho}{1+\epsilon\mathrm{e}^{\tau}})$ (dotted line). By fine-tuning the parameter s, an admixture of the gauge mode instability quantified by ϵ was made very small, $\epsilon = -0.0085\,\mathrm{e}^{-13}$, so for times $\tau < 13$ the profile $f_0(\frac{\rho}{1+\epsilon\mathrm{e}^{\tau}})$ is practically static.

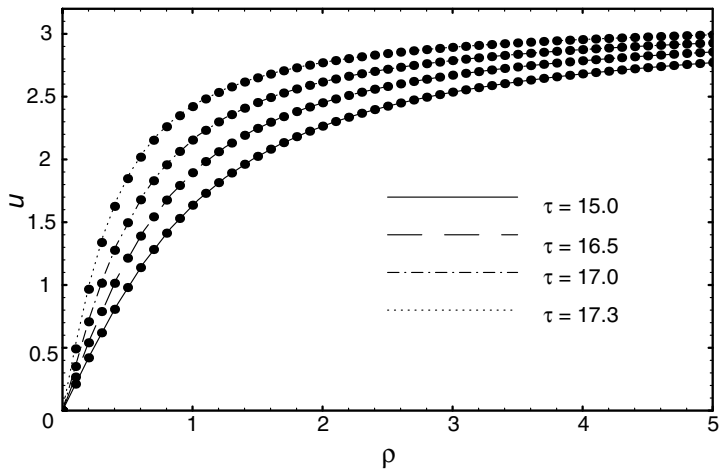

Figure 7. The same solution as in figure 6 at later times when the gauge mode instability shows up. The solution follows the moving attractor $f_0(\frac{\rho}{1+\epsilon\mathrm{e}^{\tau}})$ (dots).

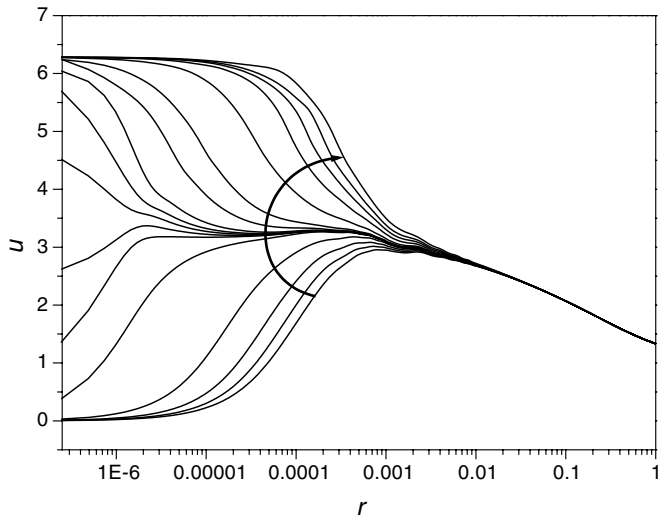

Figure 8. The last stages ($|T - t| < 10^{-5}$) of collapse of marginally supercritical initial data (the solution f_1 was gently 'pushed' towards collapse). The arrow indicates the direction of increasing time. The rapidly evolving inner region and the almost frozen outer region can be clearly distinguished — this is a typical situation in the formation of a localized singularity. The numerical solution passes through the blowup in an almost continuous manner — only the point $u(r = 0, t)$ jumps from 0 to 2π as t crosses T.

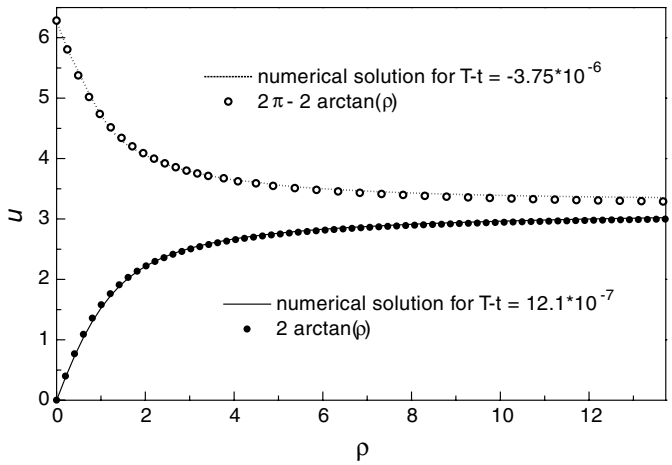

Figure 9. Evidence of universal self-similarity of blowup. The profiles just before and after the blowup are shown to coincide with the Turok–Spergel solution and its reflection.

Universality of blowup

We now address the question: what is the shape of solutions as they approach the singularity? We consider first the kink-type initial data of degree one, for example $u(0, r) = \phi(r) = \pi \tanh(r/s)$ with the ingoing-wave condition $u_t(0, r) = \psi(r) = \phi'(r)$. We found that such data always blow up in a finite time T and the asymptotic shape of solution near $r = 0$ approaches the TS solution $f_0(r/(T - t))$ as $t \to T^-$. In this sense the singularity formation can be considered as local convergence to f_0. This is shown in figures 6 and 7.

We have observed the same behaviour in other topological sectors, in particular in the case of supercritical degree zero data. In figures 8 and 9 we show the formation of a self-similar singularity in the collapse of slightly perturbed solution f_1.

On the basis of these numerical observations, we conjecture that for a large set of solutions which blow up in finite time, the asymptotic shape near the singularity is given by the self-similar solution f_0. More precisely, for such solutions there exists a time T such that

$$u(r,t) \to f_0\left(\frac{r}{T-t}\right) \quad \text{as} \quad t \to T^- \tag{27}$$

inside the past light cone of the point $(T, 0)$.

Note that in the case of self-similar blowup the energy does not concentrate at the singularity; in fact the energy inside the past light cone of the point $(T, 0)$ decreases linearly with $T - t$. This suggests that the solutions can be continued beyond the blowup time. Indeed, in figures 8 and 9 we show solutions just after the blowup. At $r = 0$ the solution $u(t, 0)$ jumps from 0 to 2π as t crosses T. Since $u = 0$ and $u = 2\pi$ correspond geometrically to the same point, namely the north pole of S^3, the solution passing through the singularity remains smooth everywhere, except at one point $(0, T)$. Moreover, the solution retains the self-similar profile at least for some time after the blowup.

5. Conclusions

We have studied the Cauchy problem for corotational wave maps from 3 + 1 Minkowski spacetime into the 3-sphere. We found that self-similar solutions play a special role in the dynamical evolution. The stable self-similar solution (Turok–Spergel solution) determines the asymptotic profile of solutions that blow up in finite time. The self-similar solution with one instability plays the role of a critical solution, that is, its stable manifold separates solutions that blow up from solutions that disperse. Of course, it is impossible to explore numerically the whole phase space, so the complete picture of singularity formation and critical behaviour might be richer than the one sketched here. In particular our analysis leaves open the question about the role of a family of static solutions. Although we have not systematically investigated the nontrivial topological sectors of the model, we anticipate a rich phenomenology of singularity formation for solutions with high degree; for example we have observed such solutions evolving (in a weak sense) through a sequence of blowup times T_i.

In our opinion the most interesting open question is: why do the large data solutions become self-similar near the singularity? We think that this problem should be approached in similarity variables in which the problem of blowup translates into a question of asymptotic behaviour as $\tau \to \infty$. Note that the evolution equation expressed in similarity variables (13) resembles the wave equation with damping. It is thus natural to seek a Lyapunov functional, that is a functional that decreases in time on solutions. If such a functional exists then its minima are the candidates for generic asymptotic states of evolution, while its saddle points are the candidates for positive codimension attractors. The self-similar solutions f_n restricted to the interval $\rho \in [0, 1]$ are the critical points of the functional

$$K[u] = \frac{1}{2}\int_0^1 \left(\rho^2 u_\rho^2 - \frac{2\cos^2(u)}{1-\rho^2}\right) \mathrm{d}\rho. \tag{28}$$

Although we were unable to show that this is a Lyapunov functional for equation (13), we believe that the mechanism suggested here is responsible for asymptotic self-similarity of blowup.

Acknowledgments

The results of this work were announced by one of us in [2] and [3]. Later, there appeared a paper by Liebling, Hirschmann and Isenberg on the same subject [9], in which criticality of the self-similar solution f_1 was also observed. This research was supported in part by the KBN grant 2 P03B 010 16.

References

[1] Äminneborg S and Bergström L 1995 On selfsimilar global textures in an expanding universe *Phys. Lett.* B **362** 39–43
[2] Bizoń P 1999 Threshold phenomena for nonlinear wave equations *Proc. NEEDS'99* (*J. Nonlin. Math. Phys.* special issue) to appear
[3] Bizoń P 2000 Equivariant self-similar wave maps from Minkowski spacetime into 3-sphere *Commun. Math. Phys.* at press
[4] Brenner M P *et al* 1999 Diffusion, attraction and collapse *Nonlinearity* **12** 1071–98
[5] Gundlach C 1998 Critical phenomena in gravitational collapse *Adv. Theor. Math. Phys.* **2** 1–50
[6] Jäger W and Kaul H 1983 Rotationally symmetric harmonic maps from a ball into a sphere *J. Reine Angew. Math.* **343** 146–61
[7] Klainerman S 1997 On the regularity of classical field theories in Minkowski spacetime *Progress in Nonlinear Differential Equations and Their Applications* vol 29 (Basel: Birkhäuser)
[8] Kovalyov M 1987 Long-time behaviour of solutions of a system of nonlinear equations *Commun. PDE* **12** 471–501
[9] Liebling S L, Hirschmann E W and Isenberg J 1999 Critical phenomena in nonlinear sigma models *Preprint* math-ph/9911020
[10] Shatah J 1988 Weak solutions and development of singularities of the $SU(2)$ σ-model *Commun. Pure Appl. Math.* **41** 459–69
[11] Sideris T 1989 Global existence of harmonic maps in Minkowski space *Commun. Pure Appl. Math.* **42** 1–13
[12] Sulem C and Sulem P-L 1999 The nonlinear Schrödinger equation. Self-focusing and wave collapse *Applied Mathematical Sciences* **139** (New York: Springer)
[13] Turok N and Spergel D 1990 Global texture and the microwave background *Phys. Rev. Lett.* **64** 2736–9